DOI: 10.21917/ijme.2026.0398

INVESTIGATION OF THERMOELECTRIC BEHAVIOR IN TI(IV) ION AND ZR(IV) ION SUBSTITUTED MN–ZN FERRITES

B. Ramesh, P. Mohan Babu, K. Devanandam, B. Venkateswarlu, S.K. Erfan and S. Kondala Rao
Department of Basic Science and Humanities, QIS College of Engineering and Technology, India

Abstract

Thermoelectric power measurements were conducted on polycrystalline Ti- and Zr-substituted Mn–Zn ferrites, and the corresponding Seebeck coefficient, carrier concentration, and drift mobility were analyzed. The Seebeck coefficient increased steadily with temperature, attaining peak values near 450 K for Ti-substituted samples and 440 K for Zr-substituted samples. All compositions exhibited n-type conduction across the entire temperature range investigated. At elevated temperatures, the ferrites demonstrated non-degenerate semiconducting behavior, indicative of thermally activated charge transport. The conduction mechanism is predominantly governed by electron hopping between Fe^{2+} and Fe^{3+} ions, in agreement with the presence of narrow energy bands and localized electronic states. The temperature-dependent behavior of drift mobility can be explained using the wavy-band model, which accounts for variations in the density of states affecting carrier transport.

Keywords:

Ferrites, Thermoelectric Power, Mobility, Carrier Concentration

1. INTRODUCTION

Ferrite materials have attracted considerable attention because of their useful electrical, magnetic, and semiconductor properties, which make them suitable for various electronic and energy-related applications. Among these materials, manganese–zinc (Mn–Zn) ferrites exhibit promising characteristics owing to their composition-dependent electrical conductivity and charge-transport behavior.

The thermoelectric properties of ferrites provide valuable information about their electronic structure, carrier type, and dominant conduction mechanisms. In particular, the Seebeck coefficient is an important parameter for understanding the relationship between temperature and charge-carrier transport. The electrical properties of Mn–Zn ferrites are strongly influenced by the distribution of iron ions, oxygen stoichiometry, and substitution of appropriate metal ions.

Substitution with titanium (Ti) and zirconium (Zr) can modify the local electronic environment and influence carrier concentration and mobility. However, the individual effects of Ti and Zr substitution on the temperature-dependent thermoelectric behavior of Mn–Zn ferrites require further systematic investigation. Understanding these effects is essential for establishing the relationship between composition, electronic states, and charge-transport mechanisms.

The present study investigates the thermoelectric power of polycrystalline Ti- and Zr-substituted Mn–Zn ferrites over the investigated temperature range. Particular emphasis is placed on evaluating the Seebeck coefficient, carrier concentration, and drift mobility as functions of temperature. The observed temperature-dependent Seebeck coefficient is analyzed to identify changes in the dominant charge-transport behavior. The consistently negative Seebeck coefficient is used to establish the n-type nature of conduction in the investigated compositions. Furthermore, the transition toward non-degenerate semiconducting behavior at elevated temperatures is examined in relation to thermally activated carrier transport. The dominant electron-hopping mechanism between Fe^{2+} and Fe^{3+} ions is considered to explain the electrical conduction characteristics. The wavy-band model is also employed to interpret the temperature dependence of drift mobility in terms of variations in the density of electronic states. Mn–Zn ferrites are widely utilized in high-frequency applications, yet detailed investigations on their charge-transport mechanisms remain limited despite several earlier studies. Among the available techniques, Hall effect and thermoelectric power (TEP) measurements serve as powerful tools for probing conduction processes. A review of the literature indicates that TEP studies on Mn–Zn ferrites are relatively scarce, although a few reports exist [1–5].

Previous work on lithium ferrites doped with non-magnetic ions such as Zn^{2+} or Cd^{2+} showed that the Seebeck coefficient (Q) exhibited a minimum at specific dopant levels, followed by an increase at higher concentrations. In contrast, Co substitution in lithium ferrites was found to enhance Q with increasing dopant levels. Similarly, Zn substitution in Mn–Zn ferrites resulted in a monotonic decrease in Q [6], whereas Zr^{4+} doping in copper ferrites caused Q to rise with concentration [7]. Studies on Sn^{4+} substitution in copper ferrite reported an initial increase in Q, followed by a decline at higher Sn levels [8], while in Sn^{4+}-doped Mn–Zn ferrites, Q increased between 0.15 and 0.30 concentration up to 440 K but decreased at higher temperatures [9]. Nb^{5+} substitution in Mn–Zn ferrites showed that Q increased up to 420 K and remained nearly constant thereafter [10]. Motivated by these varied trends, the present work aims to investigate the influence of high-valence cations (Ti^{4+}/Zr^{4+}) on the thermoelectric power of Mn–Zn ferrites.

The novelty of this study lies in the combined analysis of thermoelectric power, carrier concentration, and drift mobility in Ti- and Zr-substituted Mn–Zn ferrites within a unified temperature-dependent framework. Unlike an investigation limited to electrical conductivity or Seebeck coefficient alone, this approach connects thermoelectric response with carrier transport and the underlying electronic structure. The comparative analysis of the characteristic Seebeck coefficient maxima near 450 K for Ti-substituted ferrites and 440 K for Zr-substituted ferrites provides additional insight into the composition-dependent thermal response.

The main contribution is to clarify the relationship between transition-metal substitution, Fe^{2+}–Fe^{3+} electron hopping, and mobility variations described by the wavy-band model, thereby providing a basis for understanding and tailoring the thermoelectric and electronic properties of Mn–Zn ferrites.

2. PROPOSED METHODOLOGY

2.1 MATERIAL SELECTION AND COMPOSITION DESIGN

The proposed methodology begins with the preparation of polycrystalline titanium (Ti)- and zirconium (Zr)-substituted manganese–zinc (Mn–Zn) ferrite samples to investigate their thermoelectric and electrical transport properties. The base composition of Mn–Zn ferrite will be selected as the reference material for evaluating the effects of Ti and Zr substitution. Appropriate substitution concentrations will be designed to examine composition-dependent variations in the electronic structure and charge-carrier transport. High-purity starting materials, including manganese oxide, zinc oxide, iron oxide, titanium oxide, and zirconium oxide, will be selected according to the intended chemical composition and synthesis route. The stoichiometric quantities of the precursor materials will be calculated to achieve the desired substitution levels. Separate composition series will be prepared for Ti- and Zr-substituted ferrites to enable systematic comparison. An unsubstituted Mn–Zn ferrite sample will also be prepared as a reference wherever feasible. The selected compositions will be designed to maintain charge neutrality and minimize unwanted secondary-phase formation. The influence of substitution on iron-ion distribution will be considered during the composition-design stage. Appropriate controls will be introduced to ensure consistency across the sample series. The chemical composition and sample preparation parameters will be documented systematically. This stage will establish the experimental framework for evaluating the influence of Ti and Zr substitution on thermoelectric properties. The resulting samples will subsequently undergo structural, microstructural, and electrical characterization.

2.2 SYNTHESIS AND SAMPLE PREPARATION

The designed ferrite compositions will be synthesized using a suitable ceramic processing technique, such as the conventional solid-state reaction method. The required precursor powders will be weighed accurately according to their stoichiometric proportions. The powders will then be mixed and ground thoroughly using an appropriate milling procedure to improve compositional homogeneity. A suitable solvent may be used during wet mixing to facilitate uniform dispersion and reduce powder agglomeration. The homogenized powder mixture will be dried and subjected to preliminary calcination under controlled temperature conditions. The calcined materials will be reground to improve reaction uniformity and promote the formation of the desired ferrite phase. The resulting powders will be pressed into pellets or other suitable specimen geometries using a controlled compaction procedure. The green specimens will be sintered at an optimized temperature and duration under a controlled atmosphere. Heating and cooling rates will be maintained consistently to reduce processing-related variations. The sintered samples will be allowed to cool under controlled conditions before further processing. Their surfaces will be polished to obtain suitable contact and measurement conditions. Sample dimensions, density, and physical appearance will be recorded before electrical characterization. Multiple specimens will be prepared for each composition to improve measurement reliability. The final specimens will be labelled according to their substitution type and concentration for subsequent comparative analysis.

2.3 STRUCTURAL AND MICROSTRUCTURAL CHARACTERIZATION

The structural properties of the synthesized ferrites will be investigated to determine the effects of Ti and Zr substitution on phase formation and crystallographic characteristics. X-ray diffraction (XRD) analysis will be performed to identify the crystalline phases present in the prepared specimens. The diffraction patterns will be compared with appropriate reference data to verify the formation of the intended ferrite structure. Any additional diffraction peaks will be examined to identify possible secondary phases resulting from substitution or processing conditions. The lattice parameters will be estimated from the diffraction data to evaluate composition-dependent structural variations. Crystallite size and other relevant structural parameters may be calculated using suitable analytical methods, with their limitations clearly acknowledged. Scanning electron microscopy (SEM) will be employed to examine grain morphology, grain boundaries, and surface microstructure. Energy-dispersive X-ray spectroscopy (EDS) may be used to verify the elemental distribution and assess compositional uniformity. The grain size distribution and porosity will be examined because these features can influence carrier mobility and electrical conduction. Where available, X-ray photoelectron spectroscopy or an equivalent suitable technique will be employed to investigate the oxidation states of iron and other relevant elements. Particular attention will be given to the relative presence of Fe^{2+} and Fe^{3+} ions because their interaction is associated with electron-hopping conduction in ferrites. The structural and microstructural results will be correlated with the measured thermoelectric parameters. This analysis will help distinguish substitution-related electronic effects from changes caused by grain structure and phase composition. The characterization results will provide a foundation for interpreting the temperature-dependent transport behavior.

2.4 TEMPERATURE-DEPENDENT THERMO-ELECTRIC POWER MEASUREMENT

Thermoelectric power measurements will be conducted to determine the Seebeck coefficient of each ferrite composition over a controlled temperature range. The specimens will be placed in a suitable thermoelectric measurement system equipped with calibrated temperature sensors and electrical contacts. A controlled temperature difference will be established across the sample to generate a measurable thermoelectric voltage. The temperature gradient will be maintained within an appropriate range to ensure reliable and reproducible measurements. The generated voltage and corresponding temperature difference will be recorded after the system reaches thermal stability. The Seebeck coefficient will be calculated from the ratio of the thermoelectric voltage to the applied temperature difference, using a consistent sign convention. Measurements will be repeated at several temperatures to determine the variation of the Seebeck coefficient with increasing temperature. Particular attention will be given to the characteristic maxima observed near 450 K for Ti-substituted samples and 440 K for Zr-substituted samples, as reported in the preliminary findings. Additional

measurements around these temperatures will be performed to identify the peak positions more accurately. The sign of the Seebeck coefficient will be used to determine the dominant carrier type. The consistently negative values will be examined to verify the n-type conduction behavior of the investigated compositions. Repeated measurements will be conducted to assess experimental uncertainty and reproducibility. The resulting data will be plotted against temperature and substitution concentration. Comparative analysis will then be performed to identify the influence of Ti and Zr incorporation on the thermoelectric response. These results will provide essential information about the temperature-dependent electronic transport characteristics of Mn–Zn ferrites.

2.5 CARRIER CONCENTRATION AND DRIFT MOBILITY ANALYSIS

The carrier concentration and drift mobility of the synthesized ferrites will be evaluated using experimentally measured electrical and thermoelectric parameters. The temperature-dependent Seebeck coefficient will first be analyzed using an appropriate semiconductor transport model. Where the assumptions of a single-carrier, non-degenerate semiconductor model are satisfied, the Seebeck coefficient may be related to carrier concentration through a suitable theoretical expression. The validity of this approximation will be examined before estimating carrier concentration values. Electrical conductivity measurements will be conducted over the same temperature range using a suitable four-probe or other validated measurement technique. The measured conductivity will be combined with the estimated carrier concentration to calculate drift mobility when the adopted carrier-transport model permits this relationship. For a single dominant carrier type, mobility may be estimated from the conductivity, carrier concentration, and elementary charge. The limitations associated with localized hopping transport will be considered when interpreting mobility derived from a conventional band-transport expression. Temperature-dependent variations in carrier concentration will be investigated to identify thermally activated charge transport. The estimated drift mobility will be examined to determine whether it increases or decreases with temperature and how this behavior changes with substitution. Differences between Ti- and Zr-substituted samples will be assessed in relation to their structural and electronic characteristics. The resulting trends will be compared with the observed Seebeck coefficient and conductivity data. Appropriate uncertainty estimates will be included to avoid overstating the precision of model-derived parameters. This combined analysis will establish a consistent framework for interpreting the electrical transport behavior of the prepared ferrites.

2.6 CHARGE-TRANSPORT MECHANISM AND WAVY-BAND MODEL

The dominant charge-transport mechanism will be investigated by combining the temperature-dependent Seebeck coefficient, electrical conductivity, carrier concentration, and drift mobility results. Particular emphasis will be placed on electron hopping between Fe^{2+} and Fe^{3+} ions, which is commonly associated with electrical conduction in spinel ferrites. The possible influence of Ti and Zr substitution on local charge compensation, iron-ion distribution, and electronic localization will be evaluated using the available structural and spectroscopic evidence. Temperature-dependent conductivity data will be examined using suitable thermally activated transport models to determine whether the observed behavior is consistent with hopping conduction. Activation energies may be estimated from appropriate linear regions of conductivity-related Arrhenius plots, provided the selected model is justified. The Seebeck coefficient will also be analyzed to investigate the transition toward non-degenerate semiconducting behavior at elevated temperatures. The wavy-band model will be considered to explain mobility variations associated with spatial fluctuations in the electronic density of states and localized electronic states. Model predictions will be compared with the experimentally estimated drift mobility across the investigated temperature range. The suitability of the model will be assessed by examining the consistency between predicted and observed trends. Alternative explanations, including grain-boundary effects, compositional inhomogeneity, and changes in hopping probability, will also be considered where supported by the data. The analysis will avoid assuming that a single transport mechanism necessarily dominates at every temperature. Differences between the Ti- and Zr-substituted compositions will be used to identify possible substitution-dependent transport effects. This stage will connect the macroscopic thermoelectric response with the underlying electronic processes. The final interpretation will be based on agreement among the experimental measurements, structural evidence, and theoretical models.

3. EXPERIMENTAL DETAILS

Polycrystalline Mn–Zn ferrites with compositions $Mn_{0.58+x/2}Zn_{0.37+x/2}M_xFe_{2.05-2x}O_4$ (M = Ti^{4+}/Zr^{4+}; x = 0.05–0.25 in steps of 0.05) were synthesized by the conventional ceramic route. Stoichiometric mixtures of high-purity oxides were ball-milled, followed by calcination at 1000 °C for 3 h to ensure solid-state reaction. The calcined powders were further milled, pressed into pellets, and sintered at 1200 °C for 2 h in air. X-ray diffraction confirmed the formation of a single-phase cubic spinel structure, with the measured lattice parameter (8.5000 Å) closely matching reported values [11,12]. SEM micrographs showed uniform microstructures, indicating successful incorporation of dopants; however, more sensitive techniques such as EDX (Energy Dispersive X-rays spectroscopy) are required to reliably detect dopant distribution at low concentrations [13]. Thermoelectric power measurements were carried out using the hot-probe technique [14] over the temperature range from room temperature to approximately 650 K. In this arrangement, a heated point-contact probe acted as the hot junction, while the sample was placed on a metal base serving as the cold junction, allowing precise determination of the Seebeck coefficient.

4. RESULTS AND DISCUSSION

The thermoelectric power (Q) was determined from the thermo-emf generated due to the temperature difference between the hot and cold surfaces of the specimen. It is expressed as

$$Q = dV/dT$$

where, dV represents the induced thermo-emf across the sample corresponding to a temperature difference dT between the two surfaces of the ferrite pellet.

The Fig.1 and Fig.2 show the variation of the Seebeck coefficient with temperature for Ti^{4+}- and Zr^{4+}-substituted Mn–Zn ferrites, respectively. All samples display n-type semiconducting behavior over the entire temperature range studied. In both systems, Q increases gradually with temperature, reaching maximum values near 450 K for Ti^{4+} substitution and 440 K for Zr^{4+} substitution. At lower dopant concentrations, a slight decrease in Q is observed between 450–520 K. Beyond approximately 520 K, the Seebeck coefficient remains nearly constant for all Ti^{4+}- and Zr^{4+}-doped samples.

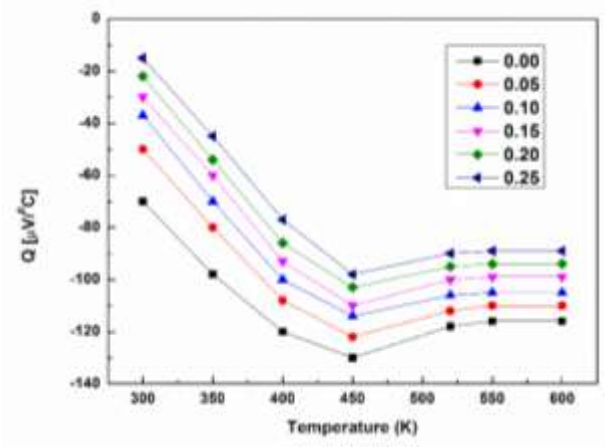


Fig.1. Negative thermoelectric power (Q) versus temperature for Ti-substituted Mn–Zn ferrite

The n-type conduction indicates that electrons are the dominant charge carriers in all compositions. The increase in the Seebeck coefficient with temperature is consistent with trends reported for other ferrite systems [7–10], and can be attributed to the rise in electron concentration and enhanced carrier mobility as thermal energy increases. The temperature dependence of Q follows the relation [15] $Q = A + (B/T)$, where A and B are constants The behavior observed below approximately 450 K for Ti^{4+}-substituted samples and 440 K for Zr^{4+}-substituted samples may be associated with extrinsic conduction processes dominating at lower temperatures before intrinsic mechanisms become significant.

Electrical conduction in ferrites is typically explained by either a hopping mechanism or a band-type process [7]. The observed decrease in the Seebeck coefficient above a certain temperature can be attributed to intrinsic conduction [16], where the contribution of electrons diminishes due to reduced hopping probability, and the thermopower becomes increasingly governed by the mobility of hole states located well below the Fermi level. At higher temperatures, the plateau observed in the Q–T curves indicates that the thermoelectric power becomes nearly temperature independent. Similar behavior has been reported for Mn–Zn ferrites [17], which are classified as degenerate semiconductors whose thermo-emf shows minimal temperature dependence. Accordingly, the present samples exhibit degenerate semiconducting behavior in the intrinsic temperature region, while at lower temperatures (extrinsic region) they behave as non-degenerate semiconductors.

Carrier concentration (n) was estimated using previously reported theoretical relations [16]. For all samples, n was found to be on the order of 10^{20} cm^{-3}, consistent with ferrites characterized by low mobility and narrow or localized electronic bands.

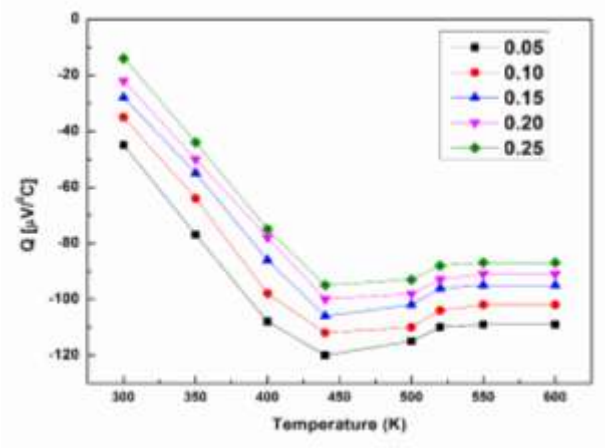


Fig.2. Negative thermoelectric power (Q) versus temperature for Zr-substituted Mn–Zn ferrite

Comparable values have been reported for other mixed ferrite systems [3–5] and specifically for Mn–Zn ferrites [9, 10]. The carrier concentration (n) exhibits a linear increase with temperature in both Ti^{4+}- and Zr^{4+}-substituted samples, consistent with previous reports on Li–Zn and Li–Cd ferrites [3, 4].

Calculation of Drift mobility from resistivity and thermoelectric power data. Mobility decreases progressively with increasing dopant concentration (x) for both Ti^{4+} and Zr^{4+} substitutions, leading to higher room-temperature resistivity. In these compositions, substitution of x/2 Mn^{2+}, x/2 Zn^{2+}, and M^{4+} ions (M = Ti^{4+}/Zr^{4+}) by 2x Fe^{2+}/Fe^{3+} ions reduces the fraction of Fe^{3+}/Fe^{2+} pairs available for electron hopping, thereby increasing resistivity. Localization of Fe^{2+} ions further contributes to this effect, as tetravalent ions form stable bonds with Fe^{2+} species during sintering [18]. Additionally, Ti^{4+} ions can function as scattering centers at the B-sites [17], hindering electron transfer between Fe^{2+} and Fe^{3+} ions and further reducing mobility.

Calculation of Drift mobility at various temperatures was conducted using conductivity data from the same samples [11] along with the evaluated carrier concentrations [18]. The mobility increases exponentially with temperature, consistent with earlier observations in Sn^{4+}- and Zr^{4+}-substituted Cu ferrites [7,8] and Sn^{4+}-/Nb^{5+}-doped Mn–Zn ferrites [9,10]. This increase is primarily attributed to the reduction in resistivity at elevated temperatures. As thermal energy increases, electron motion becomes more significant than that of holes, leading to a pronounced rise in electron mobility.

Lattice vibrations further facilitate conduction by bringing ions into closer proximity, enhancing the probability of electron transfer and thereby increasing mobility. Consequently, the temperature dependence of mobility reflects an activation energy associated with this thermally assisted process. In the present study, the activation energies derived from mobility are lower than those obtained from resistivity measurements [11]. The close agreement between activation energies derived from thermoelectric power and resistivity in the extrinsic region indicates that polaron hopping is the primary conduction mechanism.

The relevance of mobility analysis in understanding ferrite conduction has been emphasized in earlier work [16,19]. Within the framework of the wavy-band model, potential fluctuations caused by non-uniform dopant distribution and structural imperfections create localized energy wells. Carrier motion through these fluctuating potentials requires activation, giving rise to mobility-related activation energies. As these potential fluctuations become smoother, the corresponding activation energies decrease, reflecting improved carrier mobility.

5. CONCLUSIONS

The structural analysis of Ti^{4+}/Zr^{4+}-substituted Mn–Zn ferrites confirms the formation of a single-phase cubic spinel structure with no detectable secondary phases, ensuring that the thermoelectric characteristics arise solely from the intended substitutions. The temperature-dependent thermoelectric power further supports the absence of any additional phase transitions or anomalies across the studied range. Electrical transport analysis indicates electrons as the majority carriers up to 450 K, with the Seebeck coefficient varying significantly at low dopant levels and stabilizing at higher temperatures. At elevated temperatures, the samples exhibit non-degenerate semiconducting behavior, consistent with thermally activated conduction. The observed temperature dependence of the Seebeck coefficient, carrier concentration, and the associated exponent suggests the presence of narrow energy bands or localized electronic states. Additionally, the role of drift mobility in determining charge transport can be interpreted within the framework of the wavy-band model, reflecting fluctuations in the density of states inherent to these substituted ferrites.

Future research can investigate different concentrations of Ti and Zr substitutions to determine their influence on the thermoelectric properties of Mn–Zn ferrites. The effects of synthesis methods, sintering temperature, and grain size on electrical conductivity and Seebeck coefficient can be systematically evaluated. Advanced structural characterization techniques can be employed to examine phase formation, lattice distortions, and cation distribution. Temperature-dependent electrical conductivity measurements can be integrated with thermoelectric power analysis to validate the proposed charge-transport mechanisms. The relationship between Fe^{2+}/Fe^{3+} ratios and electron-hopping conduction can be explored using spectroscopic characterization techniques. Further investigations can examine the applicability of the wavy-band model across different compositions and wider temperature ranges. Computational modelling and density functional theory can be used to understand the electronic band structure and density of states. The thermal conductivity and power factor can be measured to evaluate the overall thermoelectric performance of the synthesized ferrites. Long-term thermal stability and reproducibility studies can establish their suitability for practical electronic and energy-related applications. Finally, composition optimization and experimental validation can help identify ferrite materials with improved thermoelectric efficiency and temperature-dependent charge-transport characteristics.

REFERENCES

[1] H.S. Magar, A.M. Mansour and A.M.E. Nahrawy, “Sol-Gel-Derived ZnO-Doped ZrT Oxide Nanocomposites as Highly Efficient Electrocatalysts for Nonenzymatic Hydrogen Peroxide Detection”, *Journal of Inorganic and Organometallic Polymers and Materials*, Vol. 23, pp. 1-24, 2026.

[2] H.M. James, “Conduction in Photoconductive PbS Films”, *Science*, Vol. 110, pp. 254-256, 1949.

[3] Preeti Thakur, Deepika Chahar, Shilpa Taneja, Nikhil Bhalla and Atul Thakur, “A review on MnZn ferrites: Synthesis, characterization and applications “, *Ceramics International*, Vol. 46, pp. 1-13, 2020.

[4] A.D.P. Rao, “Thermoelectric Power Studies of Sn/Nb Substituted Mn-Zn Ferrites”, *Crystal Research and Technology*, Vol. 27, No. 4, pp. 545-556, 1992.

[5] J.M. Song and J.G Koh, “Studies on the Electrical Properties of Polycrystalline Cobalt-Substituted Lithium Ferrites”, *Journal of Magnetism and Magnetic Materials*, Vol. 152, No. 3, pp. 383-386, 1996.

[6] D. Ravinder and K. Latha, “Electrical Conductivity of Mn-Zn Ferrites”, *Journal of Applied Physics*, Vol. 75, No. 10, pp. 6118-6132, 1994.

[7] B.P. Rao and K.H. Rao, “Influence of Sintering Conditions on the Microstructural and Electrical Properties of NiZn-Ferrites”, *Journal of the Magnetics Society of Japan*, Vol. 22, No. 1, pp.1-13, 1998.

[8] C. Clausell Terol, A. Barba Juan and L. Jaworska, “Enhancing NiZn Ferrite Properties through Microwave Sintering: A Comparative Study”, *Boletín de la Sociedad Española de Ceramica y Vidrio*, Vol. 63, No. 3, pp. 161-171, 2024.

[9] A.D.P Rao, B. Ramesh P.R.M Rao and S.B.Raju, “Thermoelectric Power Studies of Sn/Nb Substituted Mn-Zn Ferrites”, Journal of Material Science, Vol. 34, pp. 621-643, 1999.

[10] A.D.P Rao, “Structural, Magnetic and Electrical Studies on Sn/Nb Substituted Mn-Zn Ferrites”, Ph.D. Dissertations, Department of Electronics and Communication Engineering, Andhra University, pp. 1-125, 1995.

[11] K. Sailakshmi, B. Ramesh and S.B. Raju, “Effect of Sb^{5+}/Mo^{6+} On Magnetic properties of Mn-Zn Ferrites”, *Journal of the Magnetics Society of Japan*, Vol. 22, No. 2, pp. 37-39, 1998.

[12] M. Deepty, C. Srinivas and N.K. Mohan, “Chemical Synthesis of Mn-Zn Magnetic Ferrite Nanoparticles: Effect of Secondary Phase on Extrinsic Magnetic Properties of Mn-Zn Ferrite Nanoparticles”, *Ceramics International*, Vol. 50, No. 11, pp. 18446-18453, 2024.

[13] V.L.O. Brito, A.C.C. Migliano, L.V. Lemons and F.C.L. Melo, “Ceramic Processing Route and Characterization OF A Ni-Zn Ferrite for Application in a Pulsed-Current Monitor”, *Progress in Electromagnetics Research*, Vol. 91, pp. 303-318, 2009.

[14] D. Ravinder and K.V. Kumar, “Dielectric Behaviour of Erbium Substituted Mn-Zn Ferrites”, *Bulletin of Materials Science*, Vol. 24, No. 5, pp. 505-590, 2001.

[15] R. Satyanarayana and S.R. Murthy, "The Effect of Silica Substitution on Electrical Conduction in Nickel Ferrite", *Crystal Research and Technology*, Vol. 20, No. 5, pp. 701-715, 1985.

[16] F.J. Morin, "Electrical Properties of α-Fe 2 O 3", *Physical Review*, Vol. 93, No. 6, pp. 1195-1213, 1954.

[17] B.V. Bhise, V.C. Mahajan and S.A. Patil, "Electrical-Properties of Mn2-Zn FerriteS (TI4+ Substituted NI)", *Indian Journal of Pure and Applied Physics*, Vol. 33, No. 8, pp. 459-462, 1995.

[18] S. Singh, P. Chauhan and N.J. Singh, "Feasibility of Grid-Connected Solar-Wind Hybrid System with Electric Vehicle Charging Station", *Journal of Modern Power Systems and Clean Energy*, Vol. 9, No. 2, pp. 295-306, 2020.

[19] H. Li, H. Liu, A. Ji and Y. Jia, "Design of a Hybrid Solar-Wind Powered Charging Station for Electric Vehicles", *Proceedings of International Conference on Materials for Renewable Energy and Environment*, Vol. 3, pp. 977-981, 2013.

[20] N.B. Kumar, M.U.M. Rao, J. Veeranjaneyulu, B.M. Chandra and P.M. Venkatesh, "An Optimized Superconducting Magnetic Energy Storage for Grid-Connected Systems", *Journal of New Materials for Electrochemical Systems*, Vol. 27, No. 1, pp. 52-59, 2024.

[21] O.P. Suresh, C.S. Reddy, B.M. Chandra and B.V. Prasanth, "Economic Analysis of Grid-Tied Hybrid Solar Wind System with Electric Vehicle CS using COA-QNN Approach", *Journal of Energy Storage*, Vol. 100, No. 1, pp. 113448-113459, 2024.